Journal of Power Sources 211 (2012) 19–26

Contents lists available at SciVerse ScienceDirect

Journal of Power Sources

journal homepage: www.elsevier.com/locate/jpowsour

Novel positive electrode architecture for rechargeable lithium/sulfur batteries

Céline Barchasz [a,b,*], Frédéric Mesguich [a], Jean Dijon [a], Jean-Claude Leprêtre [b,**], Sébastien Patoux [a], Fannie Alloin [b]

[a] French Atomic Energy and Alternative Energy Agency (CEA), Laboratory of Innovation for New Energy Technologies and Nanomaterials (LITEN), 17 rue des Martyrs, 38054 Grenoble Cedex 9, France

[b] Laboratoire d'Electrochimie et Physicochimie des Matériaux et Interfaces (LEPMI), UMR 5250, Grenoble-INP, CNRS, Université de Savoie, Université Joseph Fourier, 1130 rue de la Piscine, BP75, 38402 Saint Martin d'Hères, France

ARTICLE INFO

Article history:
Received 30 November 2011
Received in revised form
6 February 2012
Accepted 18 March 2012
Available online 10 April 2012

Keywords:
Rechargeable batteries
Lithium/sulfur cells
Positive electrode morphology
Porous current collectors
Electrochemical performances

ABSTRACT

The lithium/sulfur battery is a very promising technology for high energy applications. Among other advantages, this electrochemical system has a high theoretical specific capacity of 1675 mAh g^{-1}, but suffers from several drawbacks: poor elemental sulfur conductivity, active material dissolution and use of the highly reactive lithium metal electrode. More particularly, the discharge capacity is known to be dictated by the short lithium polysulfide precipitation. These poorly soluble and highly insulating species are produced at the end of discharge, and are responsible for the positive electrode passivation and the early end of discharge. Nevertheless, the discharge capacity can be improved by working on the positive electrode specific surface area and morphology, as well as on the electrolyte composition. In this paper, we focused on the positive electrode issue. To this purpose, various current collector structures have been tested in order to achieve a high positive electrode surface area and a stable morphology during cycling. We demonstrated that the discharge capacity could be increased up to 1400 mAh g^{-1} thanks to the use of carbon foam. As well, the capacity fading could be dramatically decreased in comparison with the one obtained for conventional sulfur composite electrodes.

1. Introduction

The development of rechargeable batteries has received an increasing attention due to the growth of portable devices energy consumption. Lithium-ion battery is one of the most popular electrochemical storage systems due to high energy density, high operating voltage and low self-discharge [1]. However, the gravimetric energy density is known to be limited to 250 Wh kg^{-1} at the cell level, which is not enough to meet the electric vehicle requirements for extended range. Moreover, cobalt, which is used in commercial batteries, is toxic and expensive, and layered oxides usually have safety concerns [2].

Elemental sulfur is a promising positive electrode material for lithium batteries due to its high theoretical specific capacity of about 1675 mAh g^{-1}, much greater than the 100–250 mAh g^{-1} achievable with the conventional lithium-ion positive electrode materials [3]. The average discharge potential is around 2.1 V, and the complete lithium/sulfur (Li/S) system should allow to reach a gravimetric energy density close to 500 Wh kg^{-1}. In addition, elemental sulfur is readily available and non toxic, advantages that should allow to produce cheap and safe high energy batteries [4]. All these features explain quite well the increasing number of communications on that topic.

The sulfur reduction is a multistep electrochemical process that involves different intermediate species [5,6]. Lithium metal reacts with elemental sulfur (S_8) to produce lithium polysulfides with a general formula Li_2S_n ($2 \leq n \leq 8$). The first polysulfides that are produced have a long chain length, such as Li_2S_8 and Li_2S_6. Along the discharge, this polysulfide chain length is shortened as the sulfur is being further reduced. At the end of discharge, the final product is lithium sulfide (Li_2S), and the overall reaction equation is [7]

$$16\,Li + S_8 \rightarrow 8\,Li_2S$$

This technology has attracted attention of the electrochemistry community for many years [4,8]. However, several drawbacks still

* Corresponding author. French Atomic Energy and Alternative Energy Agency (CEA), Laboratory of Innovation for New Energy Technologies and Nanomaterials (LITEN), 17 rue des Martyrs, 38054 Grenoble Cedex 9, France. Tel.: +33 438 78 91 62; fax: +33 438 78 51 98.

** Corresponding author. Tel.: +33 476 82 65 62; fax: +33 476 82 67 77.

E-mail addresses: celine.barchasz@cea.fr (C. Barchasz), jean-claude.lepretre@ujf-grenoble.fr (J.-C. Leprêtre).

0378-7753/$ – see front matter © 2012 Elsevier B.V. All rights reserved.
doi:10.1016/j.jpowsour.2012.03.062

exist. Indeed, sulfur and lithium sulfide are highly insulating materials [9,10], and the positive electrode must contain enough of electronic conductor material, such as carbon or metallic element. To benefit from the presence of this additive, it has to be well-dispersed in the composite. Sulfur and lithium polysulfides are also soluble in organic electrolytes [11]. They can spontaneously diffuse through the liquid electrolyte, thus leading to lithium metal corrosion and self-discharge, and to an increase in the electrolyte viscosity [12,13]. At the opposite, the reduced compounds, *i.e.* Li_2S_2 and Li_2S, are insulating and insoluble. Thus, they may form a passivation layer on both positive and negative electrodes [14–16]. For these reasons, the sulfur utilization is usually very low, and the cycle life of Li/S cells is poor. Finally, the use of a lithium metal negative electrode is known to be an issue for a large-scale commercialization, as it may lead to dendrite formation, shorts-circuits and explosions.

Different strategies can be found in the literature to improve the Li/S cell electrochemical performances. Regarding the cathode side, carbon–sulfur composites can be prepared so as to trap the sulfur and lithium polysulfide compounds [17–21]. The use of mesoporous or nanostructured carbon materials enables to decrease the shuttle mechanism as well as the self-discharge, by preventing sulfur compounds from diffusing through the electrolyte. The authors indeed report a high discharge capacity along with an improved cycle life using such carbon materials. However, they finally point out that lithium polysulfides may diffuse progressively, whatever is done on the positive electrode morphology and/or on its composition [17,18]. Moreover, the use of these nanostructured carbon materials requires the vaporization of sulfur into the carbon micro porosities, which leads to strong interactions between sulfur and carbon and results in a decrease of the cell potential [21]. Other papers suggest the coating of active material using polyaniline for example [22,23]. According to authors, this treatment allows to improve both discharge capacity and fading by preventing the contact between elemental sulfur and electrolyte. Another strategy consists in studying the electrolyte composition. Many studies have been carried out on the optimization of liquid electrolyte compositions. The discharge capacity can be increased thanks to the use of ether-based electrolytes [24–26]. Additives can also be added within the electrolyte to improve the battery performances [8,27,28].

Previous works report that the discharge capacity is governed by the precipitation of short lithium polysulfides, which induces the positive electrode passivation [14–16,29,30]. It was demonstrated that the discharge capacity is dictated by the positive electrode morphology and its specific surface area [29]. Thus, this study was focused on the investigation of the positive electrode morphology impact on both cell capacity and cyclability. Two approaches were considered in this paper, either to further understand the Li/S cell functioning and limitations or to improve the electrochemical performances. In the first approach, the nature of carbon black material, which is used as a conductive additive for the sulfur composite electrodes, was investigated. Using carbons with different specific surface areas and particle sizes, we were able to point out the significant impact of the electrode morphology on the electrochemical performances. In the second approach, the starting system was not composed as usual of a composite sulfur electrode. An innovative cell design was considered to improve the Li/S cell electrochemical performances.

In the literature, the lithium battery current collectors are generally metallic foils of aluminum, copper or stainless steel [1]. They can also be made of carbon or metal-coated polymer layers, such as poly(ethylene terephthalate) (PET) or polyamide (PA) [31]. These current collector foils are then coated with the active material, as for example by doctor blade coating technique [29]. On the contrary, porous metallic current collectors are not commonly used in lithium batteries, even if conventionally used in other battery technologies, as for example nickel/cadmium or nickel/metal hydride batteries [32]. Regarding Li/S cells, there are only a few publications dealing with the use of such porous current collectors [4,33]. In this paper, a non-conventional cell design was considered to improve the Li/S cell electrochemical performances. The active material was introduced in the electrolyte through the dissolution of lithium polysulfides. As using such a catholyte [33], a rigid and porous bare current collector could be used as a positive electrode, without any sulfur source. Various current collector structures were investigated in order to provide the positive electrode with a high surface area and a stable morphology during cycling.

2. Experimental

2.1. Composite positive electrode preparation

Bare sulfur (Refined, − 100 mesh, Aldrich) was mixed with poly(vinylidene fluoride) (PVdF 1015, Solvay) and carbon black in *N*-methyl-2-pyrrolidinone (NMP, anhydrous, 99.5%, Aldrich). The S/C/binder mixing ratio was 80/10/10 wt%. A list of the investigated carbon black materials is presented in Table 1, where some of the important characteristics are summarized. Super P® (SP) carbon material was purchased from Timcal and the corresponding composite sulfur electrode refers as "reference". Ketjen Black® (KB) carbon and Activated Carbon (AC) materials were purchased from AkzoNobel (EC-300J) and Pica (Picactif® BP10), respectively. After homogenization, the slurry was coated onto a 20 μm thick aluminum current collector by doctor blade technique. The resulting electrodes were dried at 55 °C for 24 h, and then cut into Ø14 mm disks and finally dried 24 h under vacuum at room temperature. The coating thickness was about 100 μm so as to obtain a 20 μm thick electrode after drying. The positive electrode area was 1.539 cm^2, and the sulfur loading was about 2 mg cm^{-2}.

2.2. Composite positive electrode-based 2-electrodes cell assembly

The Li/S cell assembly was performed in an argon-filled glove box into CR2032 coin cells. A lithium metal foil was used under as a negative electrode and a Celgard 2400® foil as a separator. A non-woven Viledon® separator (polypropylene-based membrane) foil was also added between the composite positive electrode and the Celgard® separator. The liquid electrolyte was introduced in the cell before sealing, and was composed of LiTFSI 1 mol L^{-1} and TEGDME/DIOX in a 50/50 vol%.

2.3. Porous current collectors-based 2-electrodes cell assembly

In such cell, the positive electrode was only composed of a bare rigid and porous current collector without sulfur. A list of the investigated current collector samples and their characteristics is given in Table 2. The nickel Incofoam® (Ni foam) was gracefully provided by Inco. The glassy carbon plate was gracefully provided

Table 1
Summary of the investigated carbon black materials involved in the composite sulfur electrodes and some of their important characteristics.

Name	Grade and supplier	Specific surface area (BET)/$m^2\ g^{-1}$	Particles size/nm
SP	Super P®, Timcal	60	40
KB	Ketjen Black®, EC-300J, AkzoNobel	800	30
AC	Picactif®, Pica	1900	8000–15,000

Table 2
Summary of the investigated current collector samples and some of their important characteristics.

Name	Grade and supplier	Specific surface area (BET)/$m^2\,g^{-1}$	Thickness/μm
Ni foam	Incofoam®, Inco	0.033 [36]	2000
C foam	SR Carbon plate®, Showa Denko	0.19	2000
NWC	GDL-H2315®, Freudenberg	Below detection limit	210
VACNT	CEA	120	35

by Showa Denko (SR carbon plate®) and refers as carbon foam (C foam) afterward. The non-woven carbon (NWC) paper was gracefully provided by Freudenberg (GDL-H2315®). The dense forest of vertically aligned carbon nanotubes (VACNT) was synthesized by CEA co-workers [34]. The VACNT growth was performed on aluminum coated-silicon wafer substrates, at 580 °C using a hot-wall CVD technique and iron catalyst.

The active material was introduced in the electrolyte composition through lithium polysulfide dissolution. To this purpose, lithium polysulfides were synthesized by mixing the proper amount of elemental sulfur and lithium metal in either tetraethylene glycol dimethyl ether (TEGDME, 99%, Aldrich) or polyethylene glycol dimethyl ether (PEGDME, $M_n \approx 250\,g\,mol^{-1}$, Aldrich) so as to reach a 1 mol L^{-1} concentration of equivalent Li_2S_6 (TEGDME-based electrolytes) or Li_2S_8 (PEGDME-based electrolytes). After stirring for 48 h, all products were dissolved, giving a dark brown and viscous solution.

Two liquid electrolytes were prepared by mixing the polysulfide-containing solutions (either dissolved in TEGDME or PEGDME) with 1,3-dioxolane (DIOX, anhydrous, 99.8%, Aldrich) in a volume ratio 50/50. Lithium bis(trifluoromethane sulfone)imide (LiTFSI, 99.95%, Aldrich) was used as a lithium salt and was dissolved at 1 mol L^{-1} in the mixed solvents. Lithium nitrate ($LiNO_3$, 99.99%, Aldrich) was used as an additive to improve the coulombic efficiency [8,27] and was dissolved at a 0.1 mol L^{-1} concentration. The final polysulfide-containing electrolyte compositions were LiTFSI 1 mol L^{-1} + $LiNO_3$ 0.1 mol L^{-1} + equivalent [Li_2S_6 or Li_2S_8] 0.5 mol L^{-1} + [TEGDME or PEGDME]/DIOX 50/50 vol%. The porous current collector-based 2-electrodes cells were then assembled as above-described. The discharge capacities were calculated in mAh g^{-1} of sulfur by taking into account the amount of active material dissolved in the electrolyte.

2.4. Characterization techniques

The structure and morphology of the current collectors were analyzed by Scanning Electron Microscopy (SEM, Philips® XL30 and Leo® 1530 FEG). Specific surface area and particles size analyses were also performed (BET method, Nitrogen-Krypton, Micromeritics®, Tristar II 3020 and Malvern® MasterSizerS respectively). Electrochemical tests were monitored on the 2-electrodes cells using an Arbin® battery cycler between 1.5 and 3.0 V at room temperature.

3. Results and discussion

3.1. Material characterizations

The positive electrode morphology and its specific surface area could be modulated using different carbon black materials. Indeed, as being the major component remaining on the positive electrode after the active material dissolution process, the carbon material strongly influences the positive electrode morphology during cycling. A high surface-area additive should increase the electrode surface area remaining after sulfur dissolution. Different carbon materials were involved in the composite sulfur electrodes. Their characteristics are summarized in Table 1. Super P® carbon black is classically employed in lithium battery electrodes, because of its fine particle size of about 40 nm. It can be well-dispersed within the composite electrode materials, thus allowing the formation of an efficient percolating network using low additive contents. The Ketjen Black® material has a particle size of about 30 nm, and shows an increase in its specific surface from 60 $m^2\,g^{-1}$ for Super P® to 800 $m^2\,g^{-1}$ for Ketjen Black®. The decrease in the particle size (30 nm instead of 40 nm) cannot explain the large increase of surface area. Indeed, this increase is also due to internal porosity, with pore sizes below 10 nm. Activated Carbon is also known for its high specific surface area due to its meso and micro porosities. In this material, the BET surface area is not linked to the grain size (up to 10 μm), but rather linked to the meso and micro porosities. Thus, this study considered two kinds of high BET materials: the nano-sized one, *i.e.* the Ketjen Black®, and the micron-sized one involving nano-sized porosities, *i.e.* the Activated Carbon.

Table 2 summarizes the current collector characteristics. The corresponding SEM images are presented in Fig. 1. In Fig. 1a, the porous and highly open structure of the Ni foam is clearly visible. As also distinctly noticeable (b), the C foam presents a less open structure than the Ni one, while the specific surface is increased from 0.033 to 0.19 $m^2\,g^{-1}$. The VACNTs structure is nicely pointed out by the SEM picture (c). As-called by authors, the carbon nanotubes (CNT) "forest" is quite dense, showing a narrow CNT arrangement. The CNT dimensions are 5 nm in diameter and 35 μm in length, but they tend to agglomerate into bundles of 15 nm in diameter, spaced of about 60 nm. The VACNT substrate was implemented to provide the current collector with a high specific surface area, as providing about 350 $m^2\,g^{-1}$ (and only 120 $m^2\,g^{-1}$ if taking into account the formation of CNT bundles). The NWC paper (d) is composed of carbon fibers of about 20 μm in diameter and more than 1 mm in length. As found to be below the detection limit, its specific surface area is quite low (below 0.05 $m^2\,g^{-1}$).

3.2. Electrochemical characterizations of the 2-electrodes cells based on the use of composite positive electrodes

The impact of the electrode morphology on the electrochemical performances could be investigated by focusing on the carbon additive. As previously mentioned, the commonly used Super P® (SP) carbon black was replaced by Ketjen Black® (KB) and Activated Carbon (AC) materials, and the corresponding electrochemical results are presented in Fig. 2. As evidenced by the first discharge profile, the AC leads to a decrease in the electrochemical performances (600 mAh g^{-1} instead of 800 mAh g^{-1} obtained for the first discharge of a SP-based cell in a TEGDME-containing electrolyte at C/10 rate). On the other hand, the KB enables the capacity to be increased, as providing more than 950 mAh g^{-1} during the first discharge. Thanks to the decrease of the particles size, and the presence of micro porosities, the KB-based electrode surface area is assumed to be higher, even after sulfur dissolution, than that obtained for the SP-based one. As a result, the amount of passivation products that can be deposited on the electrode at the end of discharge could be increased, and the full electrode passivation can be delayed. On the contrary, the AC shows larger particle size along with meso and micro porosities. Surprisingly, despite the AC high specific surface value, the complete electrode passivation may not be delayed. Thus, it can be assumed that these micro and meso porosities may not be involved in the precipitation process due to their weak accessibility. The pores size may not be large enough to allow the polysulfides to quickly diffuse, and to homogeneously precipitate in the porous volume. As a conclusion, this approach

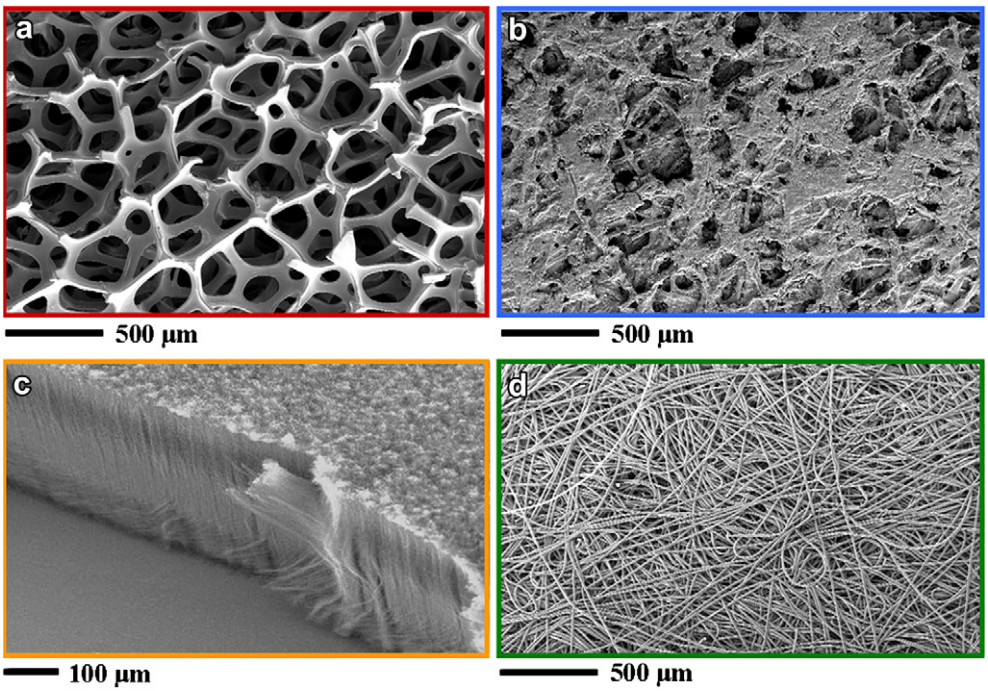

Fig. 1. SEM images of the investigated current collector samples. Upper left (a), the Ni foam image, with the courtesy of Inco. Upper right (b), the C foam image, with the courtesy of Showa Denko. Lower left (c), the VACNT image, with the courtesy of J. Dijon and co-workers. Lower right (d), the NWC image, with the courtesy of Freudenberg.

enables to conclude that the amount of species that could be deposited on the positive electrode at the end of discharge is rather linked to the carbon grain size rather than to its BET surface area.

The change in carbon black material does not have a significant role on the cycle life. As the fading may be linked to the electrode pulverization, the carbon particle size and its specific surface area do not have a relevant impact on the resulting electrode morphology after one cycle. No matter which carbon additive is involved in the electrode composition, the morphology changes would be the same during cycling (sulfur dissolution and lithium polysulfide precipitation), and the electrode pulverization would occur anyway. As a matter of fact, and despite the interesting features of KB, the corresponding cell shows only 500 mAh g^{-1} after 20 cycles. As a conclusion, the KB carbon proves to be the most powerful material to improve the Li/S cell capacity. However, the resulting capacity still remains relatively low as compared to other reported developments [19–23], and this approach does not allow to significantly improve the electrochemical performances. To this purpose, a novel electrode architecture was developed based on the use of porous current collectors as positive electrode.

3.3. Electrochemical characterizations of the 2-electrodes cells based on the use of porous current collectors

As previously mentioned, this novel Li/S cell architecture was aimed at using a rigid structure for the positive electrode while

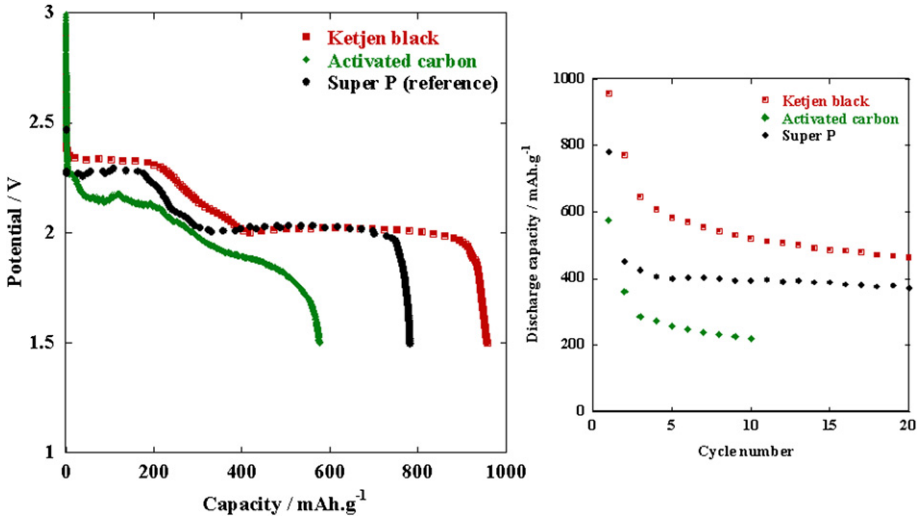

Fig. 2. First cycle profile and capacity fading of the sulfur composite electrodes performed in a TEGDME-containing electrolyte at C/10 rate. The positive electrodes were prepared with different carbon black materials in order to play on the particles size and specific surface of the conductive additive. The capacities are given in mAh g^{-1} of sulfur material contained in the positive electrode.

introducing the active material source in the electrolyte. The second discharge profile and capacity fading of the Ni foam and NWC-based Li/S cells are presented in Fig. 3, and compared to the one obtained for the reference composite electrode. The first cycle profile is not presented, as non representative of the actual capacity. Indeed, the active material was introduced through the dissolution of lithium polysulfide in the current collector-based cells. As a matter of fact, the first charge/discharge enabled to convert the lithium polysulfides into S_8. After this first cycle, the system was fully charged and the practical cell capacity could be determined during the following cycles.

Looking at the NWC electrochemical performances, the cycled capacity does not present any improvement in comparison with the conventional composite electrode. Only 450 mAh g^{-1} of sulfur could be obtained for both systems. The first discharge capacity is even smaller for the NWC-based cell, as the reference one enables to reach close to 800 mAh g^{-1}. The specific surface area of this current collector may be too low (even not quantified as below the detection limit). As a matter of fact, this NWC structure may not allow to delay the positive electrode passivation, and the resulting discharge capacity is quite low. However, this flexible current collector allows to maintain a stable capacity for many cycles (400 mAh g^{-1} obtained after 25 cycles). On the contrary, despite its high first discharge capacity, the reference composite electrode suffers from a huge capacity fading during the first cycles.

Regarding the Ni foam sample, the discharge capacity could significantly be increased in comparison with the conventional composite electrode, as about 800 mAh g^{-1} is obtained for the second cycle. The cycle life was simultaneously improved, as more than 500 mAh g^{-1} remains after 25 cycles. This current collector provides the electrode with a high specific surface area along with a stable morphology during cycling, which conveniently explain the improvement of capacity retention.

These interesting stability features can be further explained by looking at the positive electrode morphology after cycling (Fig. 4). Fig. 4a shows the initial morphology of the bare composite positive electrode. A large modification of the electrode morphology during cycling is observed (Fig. 4b), because of the active material dissolution. When elemental sulfur is dissolved, the electrode structure may collapse and some carbon particles can be released in the electrolyte (no more electronic contacts with the current collector). In addition to this dissolution, a precipitation process occurs at the end of discharge, which may account for the electrode morphology changes too. As a matter of fact, the cycles of dissolution/precipitation lead to the electrode pulverization and to the loss of available positive surface area during cycling.

On the other hand, the cycled current collectors seemed not to be damaged by the dissolution/precipitation cycles, as the morphologies presented in Fig. 4(c and d) are almost unchanged as compared to the bare current collectors (Fig. 1). Indeed, the initial porous structure still remains in the case of the Ni foam. The metallic structure may be rigid enough to accommodate the volume changes. The NWC paper is rather flexible, and may also allow the volume changes to be accommodated during cycling, enabling to efficiently decrease the capacity fading.

By changing the electrolyte composition, it was possible to further improve the discharge capacity of these current collector-based cells. Indeed, the electrolyte solvents govern the lithium polysulfide solubility, and can be well-chosen to delay the short polysulfide precipitation. To this purpose, PEGDME-like solvents have been reported to increase the lithium polysulfide solubility, especially for Li_2S_2 and Li_2S, thanks to their high solvation ability [30]. The first discharge capacity could be increased by using a Li_2S_8-containing electrolyte, thus introducing the sulfur source in its highest oxidized soluble state. The corresponding electrochemical results are presented in Figs. 5 and 6. Using this PEGDME-based electrolyte, the NWC-based cell reaches a capacity of about 800 mAh g^{-1} with almost no fading for more than 10 cycles. Once again, this current collector was found to be not as good as the reference composite positive electrode during the first discharge, as more than 1000 mAh g^{-1} is obtained for this latter. However, this current collector shows higher performances than the reference one for the following cycles, as its practical capacity remains around 700 mAh g^{-1} for more than 10 cycles (85% of initial capacity), while the reference electrode falls down to about 500 mAh g^{-1} after 5 cycles only (50% of initial capacity).

Concerning the Ni and C foams, the discharge capacity could be significantly improved in comparison with the reference composite electrode. A capacity of 1400 mAh g^{-1} is obtained for the C foam (Fig. 5c), and of 1250 mAh g^{-1} for the Ni foam (Fig. 5a). As previously noticed, the discharge capacity could be linked to the current collector specific surface. Indeed, ranging from 0.033 $m^2 g^{-1}$ to

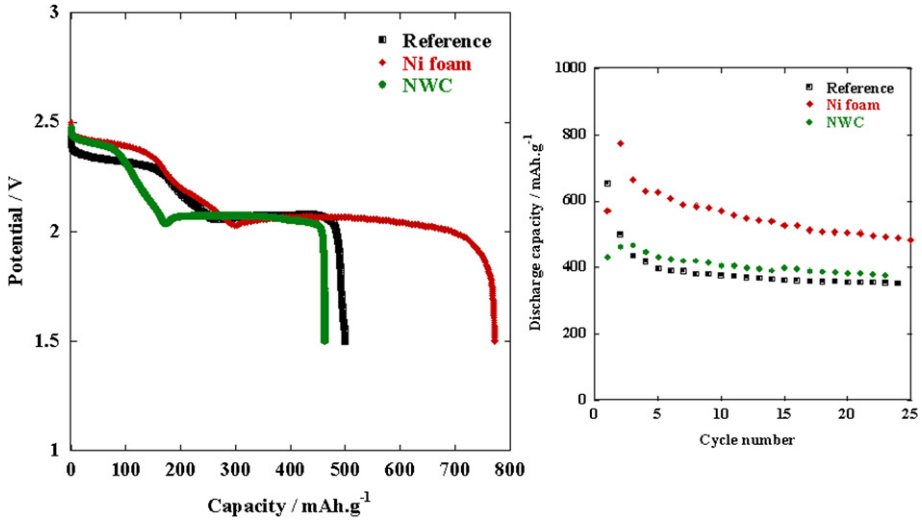

Fig. 3. Second discharge profile and capacity fading of the Ni foam and NWC-based cells performed in a TEGDME-containing electrolyte at C/100 rate. For comparison, the electrochemical performances of the reference composite electrode are also presented. The capacities are given in mAh g^{-1} of sulfur material contained in the positive electrode or in the electrolyte.

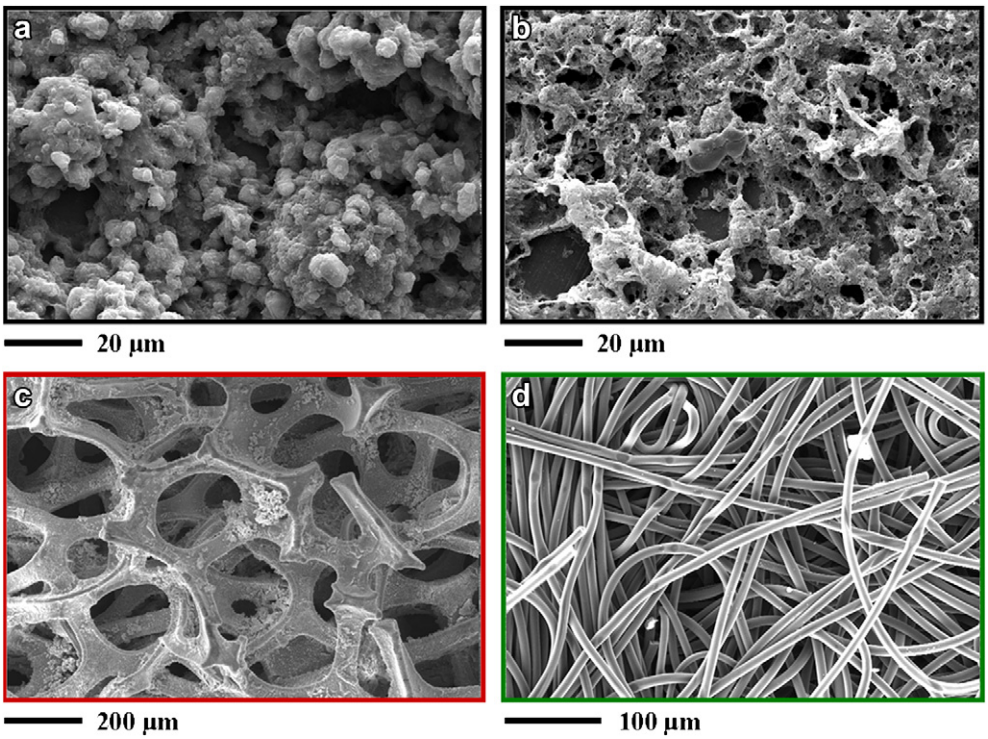

Fig. 4. SEM images of sulfur composite electrodes and current collectors before and after cycling. Upper left (a), image of the reference sulfur electrode before cycling. Upper right (b), image of the reference sulfur electrode after cycling. Lower left (c), image of the Ni foam current collector after cycling. Lower right (d), image of the NWC current collector after cycling.

0.19 $m^2 g^{-1}$, the discharge capacity could be significantly improved, thus pointing out the effect of the positive electrode morphology and surface area on the electrochemical performances. As previously concluded, the use of these morphology-stable current collectors proves to improve both discharge capacity and cycle life (85% of initial capacity remaining for all current collectors after 10 cycles).

The use of these porous current collectors does not necessarily provide the Li/S cell with an improvement of discharge capacities. In fact, depending on the collector specific surface area, a fix amount of polysulfides can be deposited on the electrode, which is not necessarily higher than the one deposited on a composite sulfur electrode during the first discharge. As an example, the NWC collector surface area is lower as compared to the one of the composite electrode (first cycle). On the other hand, with regards to the cycle life, these porous substrates enable to keep the electrode morphology stable during cycling, thus providing the same electrode surface area for all dissolution/precipitation cycles. As a consequence, the capacity fading is almost inconsistent and the discharge capacity can be maintained for many cycles (85% of initial capacity remaining after 10 cycles for all current collectors, instead of 50% obtained for conventional composite electrode). More particularly, the NWC current collector is the best one with regards to the fading. Thanks to its flexibility, the changes in active material morphology can be accommodated quite well along cycling, and this carbon paper prevents the positive electrode pulverization. Regarding the gravimetric energy density values, this was not discussed in this paper. Indeed, only commercial current collector substrates were used, which were not optimized in terms of thickness, density and porosity. Most particularly, the nickel and carbon foams were found to be quite thick and heavy, thus dramatically detrimental to the energy density. Anyway, this study enabled to point out the relationship between the collector specific surface area and the cell discharge capacity. The next step of this work would aim at improving the current collector structures, trying to optimize the thickness and the porosity for example.

3.4. VACNT substrate utilization as a porous current collector

Owing to their excellent electric, mechanical and thermal properties, carbon nanotubes have been expected to be used for many applications [35]. Dense forests of vertically aligned carbon nanotubes (VACNT) are promising materials for many applications due to their highly anisotropic and tunable properties [34]. This kind of material is not only known to be easily grown on oxide substrates like alumina, quartz or magnesium oxide, but also on conductive substrates that should be preferred for using as a current collector.

The VACNT substrate was considered owing to its atypical morphology and characteristics, providing the current collector with a high electronic conductivity, a large specific surface area (120 $m^2 g^{-1}$ if considering the CNT agglomeration) and a good mechanical strength. It was assumed to increase the available positive electrode surface area and to decrease the morphology evolution during cycling, in a view to improve both discharge capacity and cycle life. However, the corresponding electrochemical response does not fit with expectations (Fig. 7). As clearly visible, the cell polarization is quite huge, of about 0.2–0.5 V during the discharge and even 0.7 V during the charge. The discharge process had even to be performed down to 1.2 V to be completed. Nevertheless, the discharge capacity could be increased up to 1300 mAh g^{-1} for the first cycle, which is far more than the one obtained for a composite sulfur electrode.

Regarding this huge polarization, it can be explained by the substrate morphology: as the VACNT “forest” is really dense, the CNT spacing is really small (few nanometers) and the electrolyte

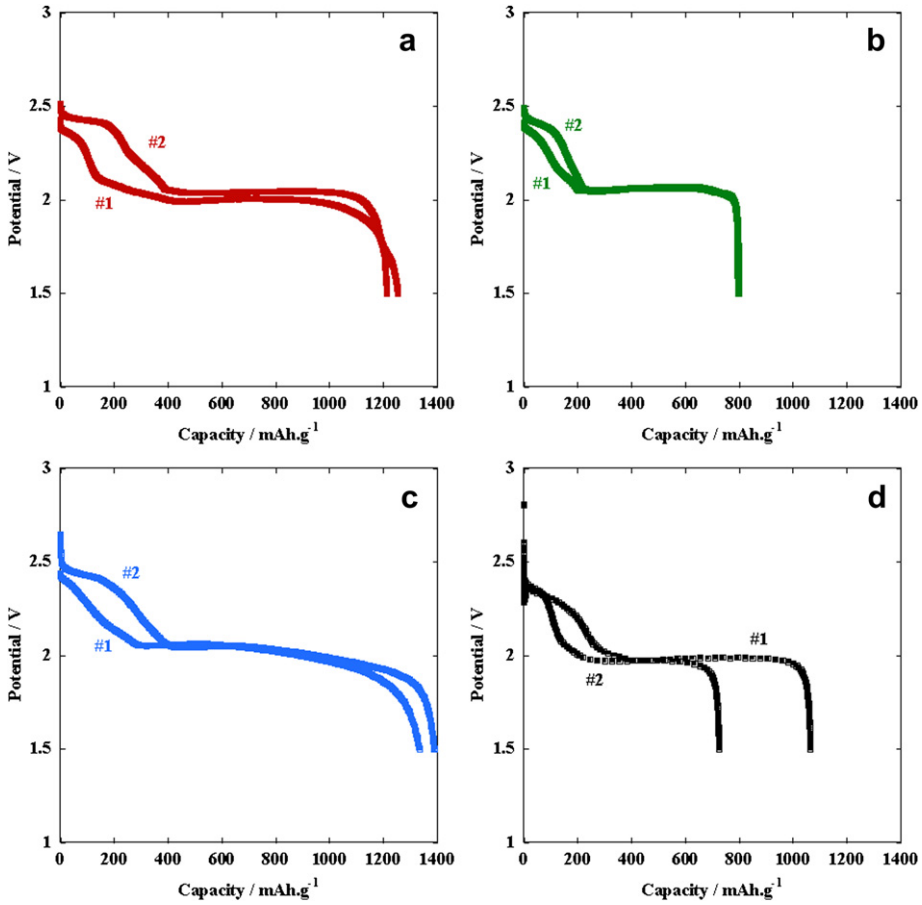

Fig. 5. First cycle profile of the Ni foam (a), NWC (b) and C foam (c) based cells performed in a PEGDME-containing electrolyte at C/100 rate. For comparison, the electrochemical performances of the reference composite electrode (d) are also presented. The capacities are given in mAh g^{-1} of sulfur material contained in the positive electrode or in the electrolyte.

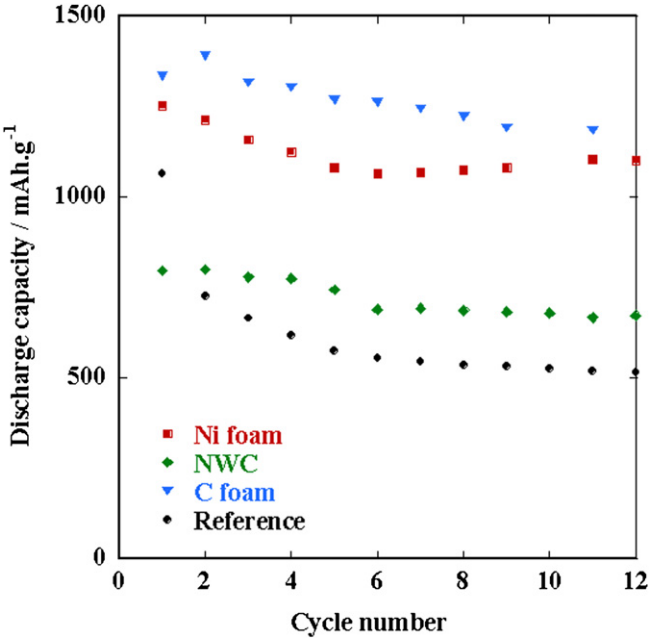

Fig. 6. Capacity fading of the Ni foam, NWC and C foam-based cells performed in a PEGDME-containing electrolyte at C/100 rate. For comparison, the electrochemical performances of the reference composite electrode are also presented. The capacities are given in mAh g^{-1} of sulfur material contained in the positive electrode or in the electrolyte.

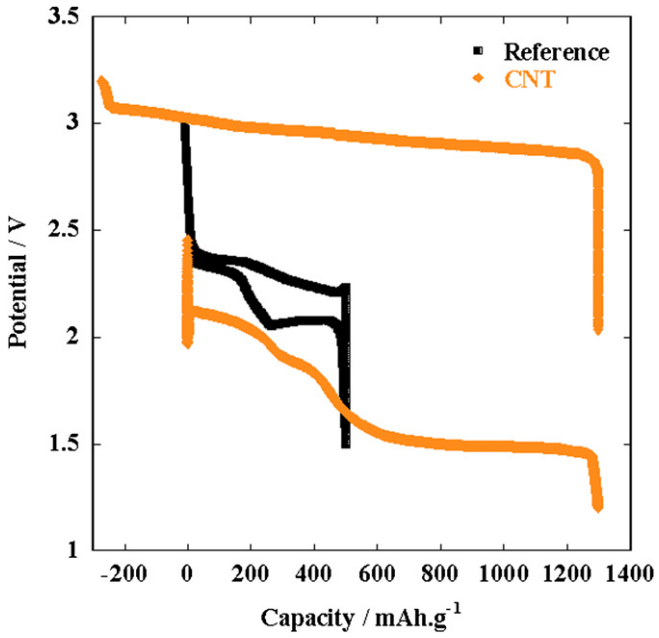

Fig. 7. Second cycle profiles of the VACNT-based and sulfur composite electrode-based cells performed in a TEGDME-containing electrolyte at C/100 rate. The capacities are given in mAh g^{-1} of sulfur material contained in the positive electrode or in the electrolyte.

diffusion through the whole electrode volume may be slowed down. This issue is even worsened if the surface tensions are significantly different between the CNT and the solvents. As a result, the ionic conductivity may be decreased in this porous structure, thus explaining this huge cell polarization.

The capacity was expected to reach the theoretical capacity of the sulfur electrode, as this current collector was providing the electrode with a huge specific surface area. However, as above-discussed, there may be some difficulties for the electrolyte to fully soak the current collector or to diffuse in the electrode channels. As the consequence, the polysulfide species may not be in contact with the whole electrode volume. The specific surface may not be entirely involved, thus explaining the incomplete sulfur utilization (1300 mAh g^{-1} instead of 1675 mAh g^{-1}). Studies are still in progress in order to improve the electrolyte and lithium salt diffusion into such dense structure. Some patterning can be attempted as well as a decrease in the density of CNT on the substrate.

4. Conclusion

The composite positive electrode composition could be improved thanks to the use of Ketjen Black® carbon material. As the particles size is decreased in comparison to the conventional Super P® carbon material, the resulting electrode surface area is expanded. The amount of lithium polysulfides that can precipitate at the end of discharge is increased, thus delaying the full electrode passivation and extending the discharge plateaus. However, the capacity of composite sulfur electrodes (casting technique) is relatively low, and the positive electrode pulverization and fading occurs during cycling in this cell architecture anyway. As a result, a non-conventional cell design was proposed in order to make an important breakthrough. To this purpose, new current collector structures have been investigated in order to provide the positive electrode with a high surface area and a stable morphology during cycling. The discharge capacity is significantly increased up to 1400 mAh g^{-1}, thanks to the use of carbon foam as a positive electrode. The capacity fading is dramatically decreased in comparison with the conventional Li/S composite electrode one (only 15% of fading for all current collectors, compared to 50% for the conventional composite electrode after 10 cycles), as the current collector structure may prevent the positive electrode pulverization. The non-woven carbon current collector proves to be the best one in providing a stable morphology along cycling, as intrinsically flexible. Last but not least, the VACNT substrate seems to be a quite promising current collector, even if there are still some needs to improve the CNT arrangement. In general, the thickness, porosity and specific surface of all current collectors should be considered with attention in the future in order to further improve the specific discharge capacity and to increase the gravimetric energy density values.

Acknowledgments

The authors would like to acknowledge the CEA-INSTN for supporting part of this study (PhD funding awarded to Céline Barchasz).

References

[1] J.-M. Tarascon, M. Armand, Nature 414 (2001) 359–367.
[2] M. Armand, J.-M. Tarascon, Nature 451 (2008) 652–657.
[3] B.L. Ellis, K.T. Lee, L.F. Nazar, Chem. Mater. 22 (2010) 691–714.
[4] R.D. Rauh, K.M. Abraham, G.F. Pearson, J.K. Surprenant, S.B. Brummer, J. Electrochem. Soc. 126 (1979) 523.
[5] H. Yamin, J. Penciner, A. Gorenshtein, M. Elam, E. Peled, J. Power Sources 14 (1985) 129–134.
[6] H. Yamin, A. Gorenshtein, J. Penciner, Y. Sternberg, E. Peled, J. Electrochem. Soc. 135 (1988) 1045–1048.
[7] Y. Jung, S. Kim, Electrochem. Commun. 9 (2007) 249–254.
[8] D. Aurbach, E. Pollak, R. Elazari, G. Salitra, C.S. Kelley, J. Affinito, J. Electrochem. Soc. 156 (2009) A694–A702.
[9] E. Peled, Y. Sternberg, A. Gorenshtein, Y. Lavi, J. Electrochem. Soc. 136 (1989) 1621–1625.
[10] Y.J. Choi, Y.D. Chung, C.Y. Baek, K.W. Kim, H.J. Ahn, J.H. Ahn, J. Power Sources 184 (2008) 548–552.
[11] H. Yamin, E. Peled, J. Power Sources 9 (1983) 281–287.
[12] J. Shim, K.A. Striebel, E. Cairns, J. Electrochem. Soc. 149 (2002) A1321–A1325.
[13] Y.V. Mikhaylik, J.R. Akridge, J. Electrochem. Soc. 151 (2004) A1969–A1976.
[14] S.E. Cheon, K.S. Ko, J.H. Cho, S.W. Kim, E.Y. Chin, H.T. Kim, J. Electrochem. Soc. 150 (2003) A796–A799.
[15] S.E. Cheon, K.S. Ko, J.H. Cho, S.W. Kim, E.Y. Chin, H.T. Kim, J. Electrochem. Soc. 150 (2003) A800–A805.
[16] V.S. Kolosnitsyn, E.V. Karaseva, Russ. J. Electrochem. 44 (2008) 506–509.
[17] X. Ji, K.T. Lee, L.F. Nazar, Nat. Mater. 8 (2009) 500–506.
[18] C. Liang, N.J. Dudney, J.Y. Howe, Chem. Mater. 21 (2009) 4724–4730.
[19] L. Ji, M. Rao, H. Zheng, L. Zhang, Y. Li, W. Duan, J. Guo, E.J. Cairns, Y. Zhang, J. Am. Chem. Soc. 133 (2011) 18522–18525.
[20] G. He, X. Ji, L. Nazar, Energy Environ. Sci. 4 (2011) 2878–2883.
[21] R. Elazari, G. Salitra, G. Gershinsky, A. Garsuch, A. Panchenko, D. Aurbach, Adv. Mater. 23 (2011) 5641–5644.
[22] F. Wu, J. Chen, L. Li, T. Zhao, R. Chen, J. Phys. Chem. C 115 (2011) 24411–24417.
[23] Y. Yang, G. Yu, J.J. Cha, H. Wu, M. Vosgueritchian, Y. Yao, Z. Bao, Y. Cui, ACS Nano 5 (2011) 9187–9193.
[24] J.W. Choi, J.K. Kim, G. Cheruvally, J.H. Ahn, H.J. Ahn, K.W. Kim, Electrochim. Acta 52 (2007) 2075–2082.
[25] W. Wang, Y. Wang, Y. Huang, C. Huang, Z. Yu, H. Zhang, A. Wang, K. Yuan, J. Appl. Electrochem. 40 (2010) 321–325.
[26] D.R. Chang, S.H. Lee, D.S. Kim, H.T. Kim, J. Power Sources 112 (2002) 452–460.
[27] J.W. Choi, G. Cheruvally, D.S. Kim, J.H. Ahn, K.W. Kim, H.J. Ahn, J. Power Sources 183 (2008) 441–445.
[28] Y.V. Mikhaylik, US Patent 2008/0193835 A1.
[29] C. Barchasz, J.-C. Leprêtre, S. Patoux, F. Alloin, J. Power Sources 199 (2012) 322–330.
[30] C. Barchasz, J.-C. Leprêtre, F. Alloin, S. Patoux, in: 218th Electrochemical Society Meeting, Las Vegas, NV, October 14–10, 2010.
[31] K. Hosaka, WO Patent 2006/061696 A2.
[32] R.J. Brodd, K.R. Bullock, R.A. Leising, R.L. Middaugh, J.R. Miller, E. Takeuchi, J. Electrochem. Soc. 151 (2004) K1–K11.
[33] S. Visco, WO Patent 2001/057943 A1.
[34] J. Dijon, P.-D. Szkutnik, A. Fournier, T. Goislard de Monsabert, H. Okuno, E. Quesnel, V. Muffato, E. De Vito, N. Bendiab, A. Bogner, N. Bernier, Carbon 48 (2010) 3953–3963.
[35] R.H. Baughman, A.A. Zakhidov, W.A. de Heer, Science 297 (2002) 787–792.
[36] M.E. Fuller, C.E. Schaefer, J.M. Lowey, Chemosphere 67 (2007) 419–427.